Journal of Applied Polymer Science

Polysaccharides Derived from Tragacanth as Biocompatible Polymers and Gels

Ali Fattahi,[1,2,3#] Paola Petrini,[4#] Fabiola Munarin,[4] Yalda Shokoohinia,[5] Mohammad Ali Golozar,[1] Jaleh Varshosaz,[3] Maria Cristina Tanzi[4]

[1]Department of Pharmaceutics, Faculty of Pharmacy, Kermanshah University of Medical Sciences, Kermanshah 6734667149, Iran
[2]Department of Materials Engineering, Isfahan University of Technology, Isfahan 84146-83111, Iran
[3]Isfahan Pharmaceutical Sciences Research Centre, Isfahan University of Medical Sciences, Isfahan 81745-359, Iran
[4]Laboratorio di Biomateriali, Dipartimento di Chimica, Materiali e Ingegneria Chimica 'G. Natta' and UdR INSTM Milano Politecnico, Politecnico di Milano, Piazza Leonardo da Vinci 32, 20133 Milano, Italy
[5]Department of Pharmacognosy and Biotechnology, Kermanshah University of Medical Sciences, Kermanshah 6734667149, Iran
[#]These authors contributed equally to this article.
Correspondence to: A. Fattahi (E-mail: a.fatahi.a@gmail.com) or P. Petrini (E-mail: paola.petrini@polimi.it)

ABSTRACT: Tragacanth gum (TG) is a natural gum whose biomedical applications are limited because of the low water solubility and the possibility to form only weak water-insoluble gels. An innovative method to produce water-soluble tragacanth (WST) is assessed in this work. WST structural characterization indicates a high-molecular weight polyuronic acid, which can undergo gelling by ionotropic complexation. Biological characterization shows no cytotoxicity on Hela, HepG2, and L929 cell lines. Furthermore, TG-based and WST-based gel beads prepared by ionic crosslinking with ferric and zinc ions are studied. Ferric WST gels exerted better cell adhesion with L929 cells than ferric alginate gels. These characteristics make WST a promising candidate for tissue engineering and drug delivery applications. © 2013 Wiley Periodicals, Inc. J. Appl. Polym. Sci. 000: 000–000, 2013

KEYWORDS: polysaccharides; polyelectrolytes; gels; biomaterials; rheology

Received 10 September 2012; accepted 14 December 2012; published online
DOI: 10.1002/app.38931

INTRODUCTION

Natural polysaccharides have attracted a rising attention in drug delivery and tissue engineering as abundant, inexpensive, hydrophilic, and biocompatible and degradable polymers. Diversity in structures and molecular weights are responsible for their variety. They can further undergo chemical and biochemical modifications.[1,2] Compared to synthetic polymers, they are more similar to the extracellular matrix, from a structural point of view and due to their high hydrophilicity. They usually induce lower inflammation reactions and cytotoxicity than synthetic materials.[3] Natural gums like gum Arabic, gum karaya, and TG are heteropolysaccharides produced by injury of the bark of plants as a consequence of a defense mechanism to prevent infections and dehydration. They have been the subject of intensive research in food industry and traditional medicine because of their simplified process of purification, low cost, availability, and their known biocompatibility considering their long time application.[4,5]

Ionic polysaccharides present interesting properties related to their polyelectrolytic nature. Positively charged polysaccharides (e.g., chitosan) and negatively charged ones (e.g., hyaluronic acid, alginate, pectin, chondroitin sulfate, heparin) can form ionically crosslinked hydrogels under mild conditions, property that is not a typical characteristic of synthetic hydrogels. The possibility to produce hydrogels under conditions that do not affect the activity of sensitive drugs, peptides, proteins, nucleic acids, and cells[1,6–8] holds a great applicative potential. Ionic polysaccharides are thus widely used for drug delivery and tissue engineering, in some cases exploiting the possibility to obtain *in situ* gelation and as model extracellular matrices for basic biological studies.[2,8–14]

Gum Tragacanth (TG), a complex mixture of different polysaccharides, contains a branched, heterogeneous, and anionic polysaccharide structurally similar to pectins. It exudates from several species of shrubs of the genus *Astragalus* mostly in certain areas of Asia and in the semi-desert and mountainous regions of Iran, Syria, Turkey.[15–17] TG has been known and used for thousands of years in texture, food, and pharmaceutical industries.[5,18] Due to unique properties of tragacanth such as acid

Additional Supporting Information may be found in the online version of this article.

and heat stability, surface activity, and emulsification ability (both of water in oil and oil in water), it has been used extensively as a stabilizer, emulsifier, and thickener in food, pharmaceutical, and cosmetic industries.[18–20] It consists of two major fractions: tragacanthin, a water-soluble fraction, and bassorin, an insoluble but water-swellable fraction.[21] The two portions of the gum consist of both tragacanthic acid, partially esterified, and arabinogalactan, but the percentage of each of them can change depending on variation of species, seasonal and geographical composition as well as mode of harvesting. Arabinogalactans, water-soluble polymers, are the major components of tragacanthin, whereas the main portion of bassorin is esterified tragacanthic acid.[21]

Despite some evidences of the use of tragacanth for drug delivery[22–24] and wound healing,[25] reproducibility, and low water solubility of TG have been restricting its use as biocompatible natural polymer in novel drug and cell delivery systems as well as tissue engineering. Recently, tragacanth hydrogels with tunable properties were developed as membranes by covalent crosslinking.[26,27]

The presence of fucose and galactose in the branches of TG polysaccharides may improve cell adhesion and cell targeting, considering that carbohydrate recognizing receptors are found on the surface of the cell; as an example, hepatocytes, alveolar macrophages, and L1210 mouse leukemia cell, are specifically bound to galactose/*N*-acetyl β-galactosamine, α-mannose, and α-fucose, respectively.[28] Fucose-containing carbohydrates and the fucosylated polysaccharides predominantly induce the differentiation of normal human keratinocytes, whereas there is no activity of these carbohydrates on cell proliferation and viability.[29] The increased elastic fiber density after topical application of fucose-containing compound to the skin of rat suggests that this is actually achieved by L-fucose and fucose-rich polysaccharides.[30] Polyanionic polysaccharides are particularly indicated to obtain systems for gradual and controlled release of cells or drugs[31] to treat or repair damaged tissues.

In this study, besides proposing a modified extraction method to produce water-soluble tragacanth (WST), the evaluation of its structural and rheological properties was conducted to assess the possibility of exploiting WST gels for such biomedical applications. Furthermore, cytotoxicity tests of WST were performed on different types of cell lines, normal and cancerous (Hela, HepG2, and L929 cell lines) with different surface receptors.

As cell or drug delivery systems recently proposed in the literature are usually in the physical form of beads, as microspheres or nanospheres to be easily injected, inhaled, or swallowed,[31] WST gel macroparticles were prepared in aqueous environment under mild conditions, as a probe of WST gel formation capability. Fibroblast L929 line was chosen for a first adhesion test in view of a possible use of tragacanth as injectable material.

EXPERIMENTAL

Preparation of WST

The procedure to obtain WST from insoluble tragacanth was modified from methods previously described in the literature.[19,21] Briefly, 1 g of tragacanth (ribbon type from *Astragalus gossypinus*, purchased from local market of Isfahan, Iran) was dispersed in 100 mL of distilled water, and the suspension was stirred overnight. NaOH was added to obtain a 0.5 *M* NaOH solution, and the mixture was stirred for 6 h at 4°C. Then the alkaline solution was neutralized by 1 *M* HCl to achieve a final pH of 7.5. The solution was centrifuged for 10 min at 6000 rpm and then filtered in sinter funnel to remove any insoluble residue. The filtered solution was concentrated by rotary evaporator at 60°C under vacuum. Absolute ethanol was added to the concentrated solution to achieve 70% v/v ethanol. The precipitate was separated by sinter funnel and it was washed by 70% ethanol and absolute ethanol three times. The final product was dried and it will be further referred as WST.

Molecular Weight Analyses

The intrinsic viscosity of WST solutions was measured using an Ostwald viscometer. The measurements were made at a temperature of 24 ± 1°C. WST (100 mg) was dissolved in 50 mL of 0.1 *M* NaCl solution at room temperature.[32] Then, 5 mL of the solution was added into the capillary viscometer, and the efflux time was measured. After each viscosity measurement, WST solution was diluted by 5 mL of 0.1 *M* NaCl. Intrinsic viscosity $[\eta]$ was determined by eq. (1).

$$[\eta] = \lim_{c \to 0} \frac{(\eta - \eta s)}{\eta s C} \quad (1)$$

where η is the solution viscosity, ηs is the solvent viscosity, and C is the solution concentration.

Size exclusion chromatography (SEC) was performed in aqueous 0.1 *M* $NaNO_3$ solution at 25°C (0.8 mL/min) using a Waters system (Waters, Milano, Italy 1515 pump) equipped with a precolumn (Ultrahydrogel Guard, 60 × 40 mm, Waters, Milano, Italy), three Ultrahydrogel columns (Ultrahydrogel 250, 500, 1000; 7.8 × 300 mm, Waters, Milano, Italy) and a refractive index detector (Waters 2414). The weight-average molecular weight (M_w) and molecular weight distribution (M_w/M_n) of WST were calculated on the basis of a pullulan calibration (Shodex Showa Denko pullulan standards, range 708–5.9 kDa, Waters, Milano, Italy). Raw TG could not be analyzed being a suspension and not a homogeneous solution.

Rheological Characterization

Rheological characterization was performed with AR 1500ex rheometer (TA Instruments, Milano, Italy), equipped with a cone-plate geometry (diameter = 2 cm, truncation = 32 mm, working gap = 32 mm). Dispersions and solutions (1%, w/v) of TG and WST, respectively, were analyzed at 25°C, with flow and oscillatory assays.

Flow ramp tests were conducted to define the linear viscoelastic region, in which the stress generated varies linearly with the applied strain. Strain ramps were performed at $F = 1$ Hz frequency over an oscillation strain of 0.1–300%.

The flow behavior was determined with shear rates in the range of 0.1–1000 s^{-1}, and viscosity curves were fitted using the non-Newtonian Carreau (eq. (2)) and Cross (eq. (3)) viscosity models.

$$\eta_\alpha = \eta_\infty + (\eta_0 - \eta_\infty)/[1 + (\tau_{CA}\dot{\gamma})^2]^M \quad (2)$$

$$\eta_\alpha = \eta_\infty + (\eta_0 - \eta_\infty)/[1 + (\tau_{CR}\dot{\gamma})^m] \quad (3)$$

where η_α is the apparent viscosity, η_0 is the zero shear rate viscosity, η_∞ the infinite shear rate viscosity, t is the time constant, while m and M are dimensionless parameters of the model.

Shear sweep tests were assessed to measure the yield stress, varying the shear from 100 s^{-1} to 0.01 s^{-1} at $T = 25°C$.

Dynamic properties were investigated with oscillatory assays, measuring the storage (G') and loss (G'') moduli in the linear viscoelastic range (LVR) at constant temperature ($T = 25$ °C), varying the angular frequency from 1 to 100 rad/s.

Determination of Galacturonic Acid and Degree of De-Esterification

The methylester and galacturonic acid content of TG and WST were determined according to the titrimetric method developed for pectins[2] of Food Chemical Codex (FCC) IV and US Pharmacopeia (USP) XXVI. Dried samples of TG or WST (500 mg) were transferred to a 250 mL flask and put in 100 mL of distilled water. After the samples were completely dispersed (in case of TG) or dissolved (in case of WST), five drops of phenolphthalein (Sigma Aldrich, Milano, Italy, 31923-6, 0.5% w/v solution in 50% w/v ethyl alcohol) was added, and the sample was titrated with 0.5 *M* sodium hydroxide. The result was recorded as the initial titer (IT). Then, 10 mL of 0.5 *M* sodium hydroxide was added, the sample was shaken vigorously and allowed to stand for 15 min; 10 mL of 0.5 *M* hydrochloric acid was added, and the sample was shaken until the pink color disappeared. The solution was titrated with 0.5 *M* sodium hydroxide to a faint pink color that persisted after vigorous shaking (end point). This volume of titration was recorded as the saponification titer (final titer, FT).[33] Degree of esterification (DE) was calculated from eq. (4).

$$\%\mathrm{DE} = 100 - [\mathrm{FT}/(\mathrm{IT}/\mathrm{FT}) \times 100] \quad (4)$$

Fourier transformed infrared (FTIR) spectroscopy

Spectroscopy

FTIR spectra were acquired in transmission mode from TG and WST powders and dried WST beads. The spectra were recorded with a Nicolet 6700 spectrometer (Thermo Electron Corporation, Italy), in the spectral range of 4000–400 cm^{-1} at a resolution of 4 cm^{-1}.

Evaluation of Gelling Behavior of TG and WST

To evaluate the possibility to prepare beads, TG and WST in different concentrations (1–4%, w/v) were dropped into the crosslinking solution (calcium chloride, ferric chloride, and zinc chloride (Merck, Germany) in different concentrations. The beads were left in the curing solution at a slow stirring to avoid agglomeration for 20–30 min. Then prepared beads were collected by nylon filter and extensively washed in water under slow stirring.

Morphological Studies

The surface and internal morphology of the crosslinked beads were examined using a scanning electron microscope (SEM, SERON technology, AIS2100). Prior to examination, the samples were lyophilized, fixed on a brass stub, and coated with a gold-palladium layer under argon atmosphere using a gold sputter module in a high vacuum evaporator. For internal morphology study, lyophilized beads were cut in sections by the sharp cutter.

Cell Culture

HepG2 (human hepatocellular carcinoma cell line), Hela (human epithelial cervical cancer cell line), and L9 29 (murine fibroblast-like cell line) were obtained from Pasteur Institute, Iran. Cells were maintained in RPMI-1640 supplemented with 10% (v/v) fetal bovine serum (FBS) and penicillin/streptomycin (50 IU ml^{-1}, 500 μg ml^{-1}) at 37°C in a humidified atmosphere containing 5% CO_2. Cells were subcultured regularly using trypsin/Ethylenediaminetetraacetic acid (EDTA).

In Vitro Cytotoxicity

To assess the cell viability of WST, a test with 3-(4,5- dimethylthiazole-2-yl)-2,5-diphenyl tetrazolium bromide (MTT, Sigma Aldrich, Italy) was performed. The MTT enters in the mitochondria of cells, and it is reduced by viable cells to formazan crystals, that produce a dark-purple color. When adding DMSO, formazan crystals dissolve and can be measured by spectrophotometry.

The cytotoxicity of WST was performed against HepG2, Hela, and L929 cell lines. Briefly, HepG2, Hela, and L929 cells were plated in 96-well plates and grown for 24 h. The cells were exposed to a serial of concentrations of WST (1–500 μg ml^{-1}), at 37°C for another 72 h. At the end of incubation time, 20 μL of MTT solution with the concentration of 5 mg/mL was added and incubated for further 3 h at 37°C. The medium containing unreacted MTT was removed, and each well was washed with 50 μL of PBS. Then 150 μL of dimethyl sulphoxide (DMSO) was added to each well to dissolve the formazan crystals. Finally, the absorbance of dissolved formazan was measured at 540 nm in an Enzyme-linked immunosorbent assay (ELSIA) reader (Bio-Rad, Model 680).[34,35] All the experiments were performed in triplicate. Statistical analyses were achieved using the SPSS software package (v.17). One-way ANOVA tests and Tukey Post Hoc test were used with a confidence level of $\alpha \leq 0.05$ to assess of statistically significant homogeneous subsets.

In Vitro Cell Adhesion Study

As substrates for cell adhesion tests, films of crosslinked WST were prepared by adding 1 mL of 1% w/v WST solution into the cell culture plate (24 wells). The solutions were dried at 60°C overnight then 2 mL of 0.25% ferric chloride was added into each well and incubated at room temperature for 6 h to crosslink WST film. To remove free ferric ions, crosslinked films were washed several times with deionized water. Alginate films were prepared as control, following the same procedure.

The plates coated by WST or alginate film were sterilized by 70% ethanol and UV light under laminar flow hood. Briefly, 2 mL of 70% ethanol was added into each well and incubated under laminar hood for 1 h and then the plate was exposed at UV light for 10 min. Finally, ethanol solution was discarded,

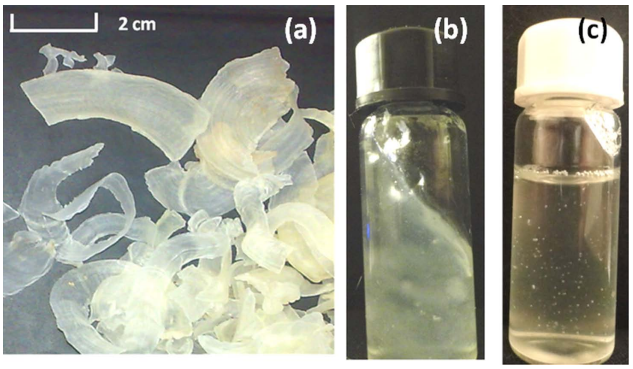

Figure 1. Ribbon type tragacanth (a), tragacanth suspension (25 mg/mL, pH 5.2) (b), and WST (25 mg/mL, pH 4.5) (c). [Color figure can be viewed in the online issue, which is available at wileyonlinelibrary.com.]

and wells were washed by sterile PBS for several times to remove any ethanol residue.

1 mL (5×10^4 cells/ml) of L929 cell suspension was added into each well, and plate was incubated in 37°C for 36 h. After that the morphology of the cells under the surface was evaluated by inverted optical microscopy and the average of the adherent cells over the total number of cells, counted in at least three images of different well plates, gave the mean percentage of cell adhesion for each sample.

RESULTS AND DISCUSSION

Preparation and Characterization of WST

Although tragacanth contains an anionic polysaccharide, tragacanthic acid, it shows only weak interactions with cationic metallic ions, therefore the formation of water-insoluble gels is prevented. Its low solubility restricts its application as biomedical polymer, as solubility is needed for many different aspects, including its modification to prepare water-insoluble gels, coatings, scaffolds, and reactions to functionalize the polymer for targeting. Whole tragacanth or the soluble part, including also neutral polysaccharides as arabinogalactan, is generally considered in food industry.[5] The insoluble part, mainly composed of cellulose, arabinogalactan, and esterified tragacanthic acid, is in some cases discarded. The extraction method proposed in this work relates to the retrieval of the esterified tragacanthic acid from the insoluble part of tragacanth in addition to the tragacanthic acid in the soluble part. The possibility to obtain COOH-rich polysaccharides is the premise for the obtainment of ionic crosslinked, water-insoluble gels.

Tragacanth ribbons [Figure 1(a)] were dispersed in water [Figure 1(b)], and the water suspension was treated with NaOH. This was aimed both to separate cellulose, not soluble in alkaline solution, and to promote the dissolution of tragacanthic esters through de-esterification by alkaline saponification. Finally, the selective precipitation in 70% (v/v) ethanol was performed to separate arabinogalactan from tragacanthic acid as WST [Figure 1(c)].

On the basis of the hypothesis of structural similarity, the chemical titration method of the methyl ester content of pectins was applied to TG and WST. Results are consistent with a low degree of esterification (94.3 ± 1.3% of de-esterified galacturonic acid) in WST comparing to TG (63.1 ± 2.8% of de-esterified galacturonic acid). Intrinsic viscosity is related to the molecular weight of the polymers by Mark-Houwink equation ($[\eta] = KM^{\alpha}$). For tragacanth from *A. gossypinus*, ribbon type, K and α were evaluated as 9.077×10^{-5} and 0.87, respectively.[19] For the isolated WST, an intrinsic viscosity of 11.95 dL/g was obtained, corresponding to an indicative molecular weight of 770 kDa. However, due to the different variables, strictly dependent on the structure of the polymers, such as interchain interactions, polydispersity, polymer/solvent interactions, and the presence of charges on the macromolecules,[32] a systematic study on this specific type of tragacanth has to be performed. SEC results indicate a chromatographic peak centered at 22 min with a polydispersity typical of low disperse polymers ($M_w/M_n = 1.9$). The peak is slightly asymmetric being broader toward higher elution times. M_w and M_n, relative to pullulan standards, were calculated as 300 and 157 kDa,, respectively.

FTIR of raw tragacanth (Figure 2) shows typical bands of polysaccharides. Asymmetric stretching of the many hydroxyl groups in TG is a broad and intense band in the spectral range of 3680–3000 cm^{-1}. Symmetric and asymmetric stretching of the different CH bonds is found in the range of 3000–2800 cm^{-1} while CH deformations are at 1437 cm^{-1}. The specific spectral features of other branched polysaccharides containing polyuronic acids, such as pectins,[36] can also be found in TG spectrum. Considering this similarity, we propose the attribution of the infrared bands (Table I). Several bands are related to the vibrational modes of COOH in galacturonic acid and its salts and esters, namely asymmetric stretching (1740–1600 cm^{-1}), symmetric stretching of carboxylate groups and methyl groups in methyl esters of galacturonic acid (1417 and 1368 cm^{-1}, respectively).

The mid-infrared region at 1300–1000 cm^{-1} [Figure 2(b)] contains ring vibrations overlapped with stretching vibrations of (C—OH) side groups and the (C—O—C) glycosidic bond vibration. Polygalacturonic acids have distinctive absorption band maxima in this region, with very strong absorptions at 1100 and 1017 cm^{-1},[36] maximum absorption bands at 1070 and 1043 cm^{-1} indicating the presence of galactose containing polysaccharides such as arabinogalactans and galactans. In this region, raw tragacanth shows the typical spectral pattern of arabinogalactans although the presence of the polygalacturonic bands is detectable (Figure 2). The presence of bands at 834 and 898 cm^{-1} indicates the presence of both α-anomer and β-anomer, respectively.

Two different structural changes can be hypothesized to explain the differences between WST and raw TG spectra (Figure 3): the basic pH of the solution in the extraction process promotes the de-esterification process of the ester groups and induces salification of the free COOH groups. Infrared spectroscopy indicates a sharp decrease of the band of C=O of COOH and COOR groups (ν_{asym} C=O at 1739 cm^{-1}) following the alkaline treatment, associated to a steep increase of intensity of carboxylate groups (ν_{asym} C=O at 1616 cm^{-1} + ν_{sym} C=O at 1417 cm^{-1}). As the disappearance of 1368 cm^{-1} peak, associated to CH_3 deformations in OCH_3 from ester groups, is observable, a

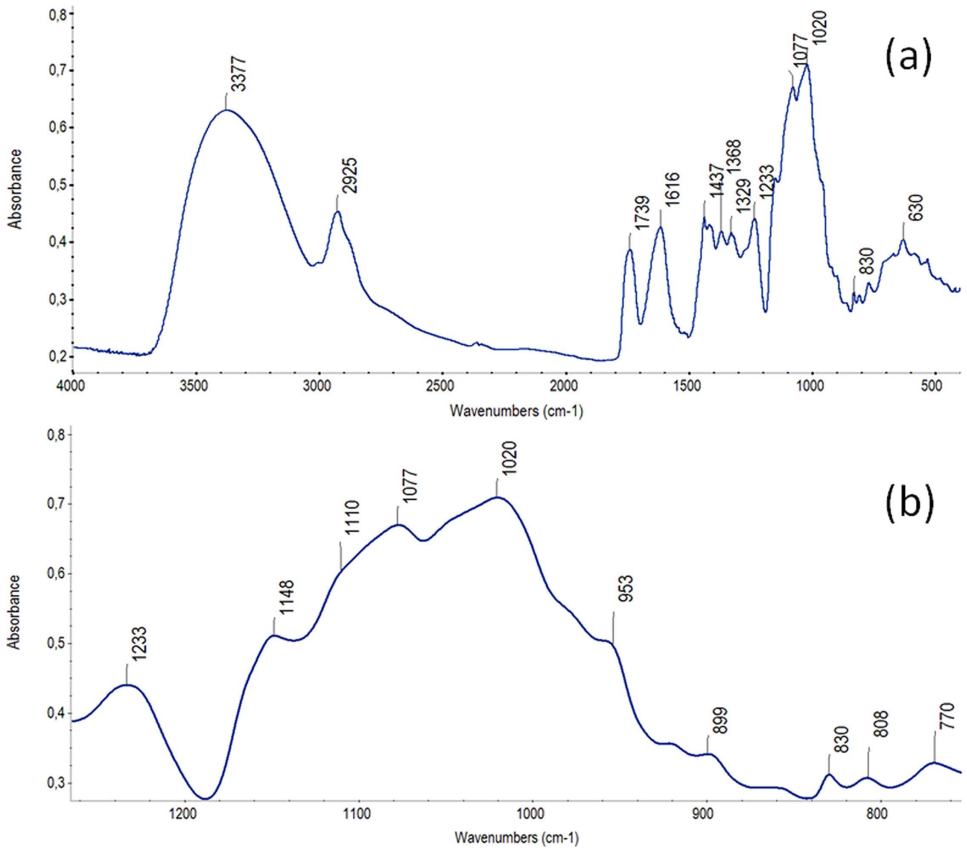

Figure 2. FTIR spectra of raw tragacanth (TG), (a) region 4000–500 cm^{-1} and (b) enlargement for the mid-infrared region at 1250–750 cm^{-1}. [Color figure can be viewed in the online issue, which is available at wileyonlinelibrary.com.]

contribution to the discussed changes in C=O stretching bands has to be found in a partial de-esterification of methyl esters of galacturonic acids. This result is consistent with the extremely high degree of de-esterification obtained from the chemical titration of WST (94.28 ± 1.31%). The slight shift toward higher frequency of ν_{asym} OH (3680–3000 cm^{-1} for TG to 3700–3030

Table I. FTIR Band Attribution for Tragacanth, WST, and Tragacanth Gels (Fe/WST)

Raw TG (cm^{-1})	WST (cm^{-1})	Fe/WST (cm^{-1})	Vibrational mode
3377	3384	3384	Asymmetric strectching of OH group (free+H-bonded)
2925	2935	2936, 2977	Asymmetric stretching of CH group
2872	2872	2872	Shoulder, symmetric stretching of CH group
1739	1739	1739	Asymmetric stretching of C=O in galacturonic acid + its esters
1616	1610	1630	Asymmetric stretching of carboxylate group
1437	-	1429	Deformations of CH group
1417	1416		Symmetric stretching of carboxylate group
1368	-	1375, 1359	Symmetric deformation of OCH_3
1273	-	1254	CH_2 twist and rock
1148	1144	1152	Stretching C—C in homogalacturonan
1110	-	-	Shoulder, C—O stretching of homogalacturonan
1077	1078, 1088	1075, 1090	Galactose containing segments (arabinogalactan, β-galactan or others)
-	1039	1042	Galactose containing segments (arabinogalactan, β-galactan or others)
1020	1021	-	Stretching C—C in homogalacturonan
953	962	972	C1-H, ring
898	898	899	β anomer
830	833	833	α anomer

Applied Polymer SCIENCE

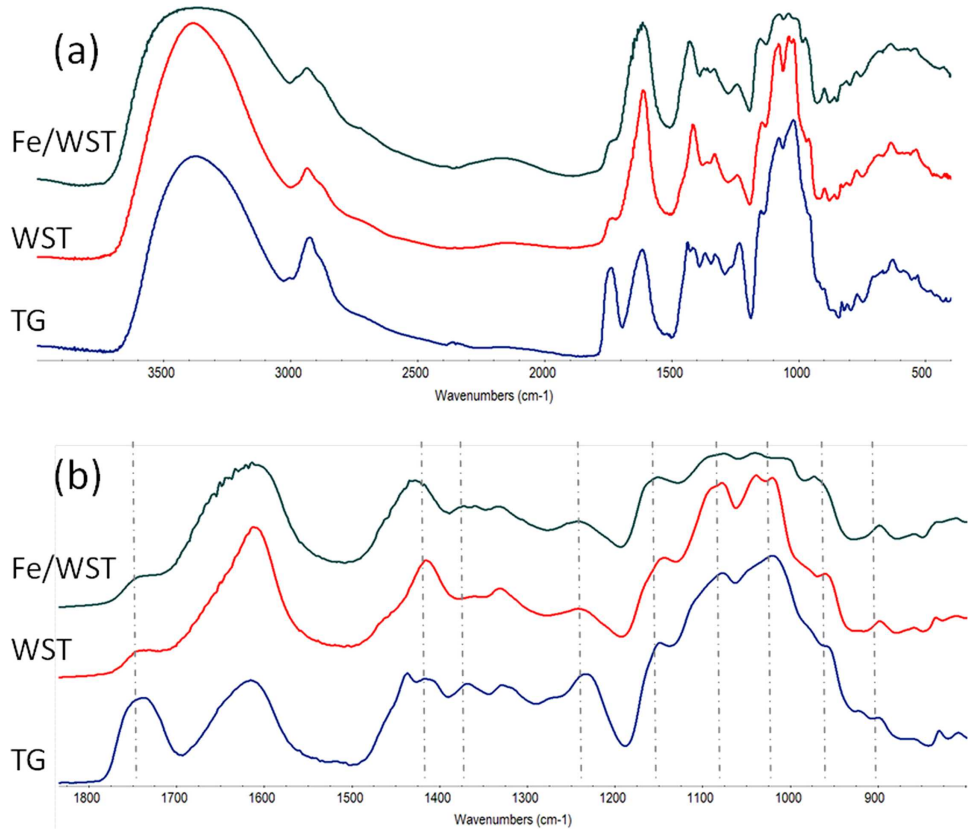

Figure 3. FTIR of raw tragancanth (bottom line, blue), WST (medium line, red), and Fe/WST (top line, green), (a) region 4000–500 cm^{-1} and (b) and enlargement for the mid-infrared region at 1250–750 cm^{-1}. Dashed lines indicate the differences in the bands. [Color figure can be viewed in the online issue, which is available at wileyonlinelibrary.com.]

cm^{-1} for WST) indicates an increase in OH groups involved in hydrogen bonding versus free OH, which can be related to the higher ionization of the polysaccharide.

Alkaline treatments typically produce unsaturated residues in case of high degree of methylation. They were not observable in our condition of analyses. The reasons can be related either to the limited extent of occurrence of β-elimination or to the overlapping of the contribution of the typical bands of unsaturated bonds with the intense bands in the same spectral areas.

Rheological Characterization

The flow and dynamic curves of TG and WST 1% (w/v) suspension and solutions are presented in Figures 4–6. From the oscillation amplitude test, it was possible to discriminate two different regions, namely a linear viscoelastic region (below 18% oscillation strain, corresponding to shear stress of 8.02 Pa and 0.18 Pa for TG and WST, respectively) in which G' and G'' were constant, and a nonlinear one (above 18% oscillation strain) in which G' and G'' started to decrease with the increase of the oscillatory strain (Supporting Information Figure A). Accordingly, flow and oscillatory tests were then performed within the linear viscoelastic domain.

Viscosity and stress of TG solutions resulted higher than the ones of WST (Figure 5) and comparable to the values found in the literature for tragacanthin solutions.[19,37] The differences observed in the flow curves can be attributed to the different physical form of the samples: TG is a suspension of insoluble microgels or nanogels, while WST is an aqueous solution. Both TG and WST exhibited a shear-thinning behavior, where the shear viscosity decreases as the applied shear rates increases. Viscosity data were fitted with the Carreau and Cross models for non-Newtonian fluids (Table II), showing optimal fitting for Carreau model.

To support the presence of shear-thinning behavior, the yield stress was investigated with shear sweep measurements (Figure 5). For non-Newtonian solutions, the viscosity displays a slope near −1 at low shear rates, which indicates the predominance of yield stress effects, and the value of the yield stress remains almost constant. The measured yield stress was 5.64 Pa for TG and 0.06 Pa for WS, in both cases comparable with the stress values at the end of the LVR.

The dynamic behavior of TG and WST is shown in Figure 6. The procedures followed to extract WST from TG caused G' and G'' values to decrease over the whole frequency range. The obtained results are in correspondence with the trend reported by other authors working in similar concentration ranges of *A. gossypinus* tragacanth.[38,39]

The storage (G') and loss (G'') moduli of TG slightly increased with frequency, with G' greater than G'' at almost all the frequency range covered, indicating a gel-like behavior of TG (Figure 6). As

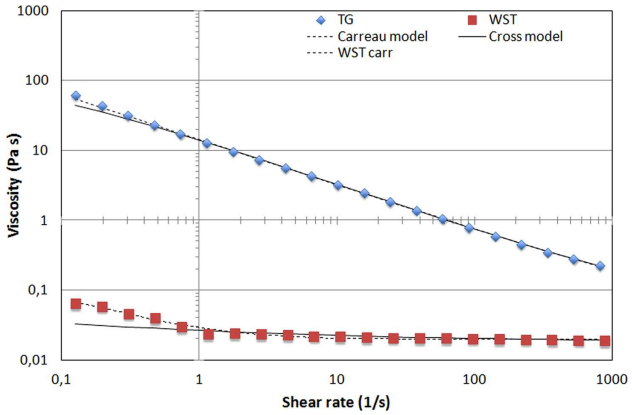

Figure 4. Viscosity of TG and WST as a function of shear rate. [Color figure can be viewed in the online issue, which is available at wileyonlinelibrary.com.]

previously discussed by Balaghi et al.,[16] this effect can be accounted to the presence of bassorin (the insoluble fraction of the gum), whose content is over 50% in *A. gossypinus* tragacanth. The entanglements of the long bassorin particles, combined to their swelling ability, are probably forming physical networks, determining the weak gel character of TG. In the extracted WST, with the absence of microgels and nanogels and the reduced molecular weight of the polysaccharides, the values of loss modulus were higher than the values of storage modulus (Figure 6) for all the considered frequencies. The viscous behavior, probably accounted to a less entangled structure, is therefore dominant in this region.

Evaluation of Gelling Behavior of TG and WST

Ionotropic gelation is typical of polyuronic acids, with the characteristics of gelation being strictly dependent upon the structural characteristics of the polysaccharides. It is mainly related not only to the degree of esterification but also to the extension of domains containing monosaccharides with carboxylic groups and their distribution along the polymeric backbone, the branching of the polysaccharidic chain, and the copresence of neutral monosaccharides and polysaccharides. From the reverse point of view, the study of gelling was performed to provide information regarding the structure of the polysaccharide. The ionotropic gelling of TG and WST was studied and compared. Different cations were considered, Fe^{3+}, Zn^{2+}, and Ca^{2+}.

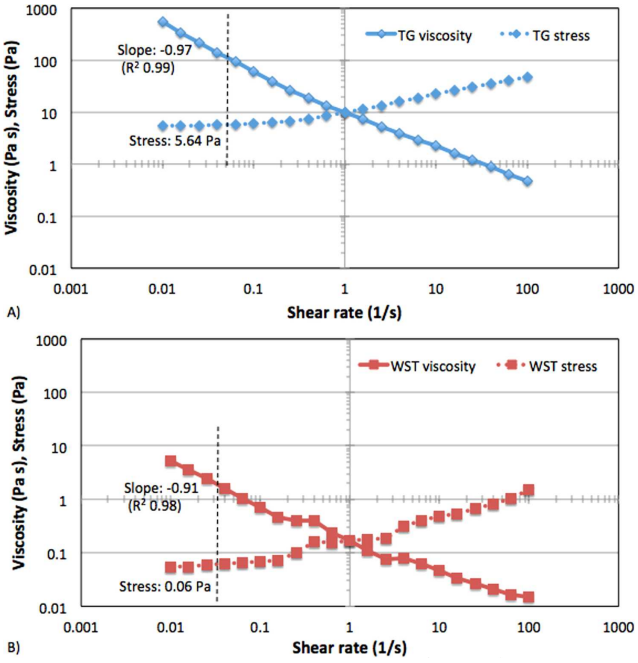

Figure 5. Yield stress of TG and WST (shear sweep test). [Color figure can be viewed in the online issue, which is available at wileyonlinelibrary.com.]

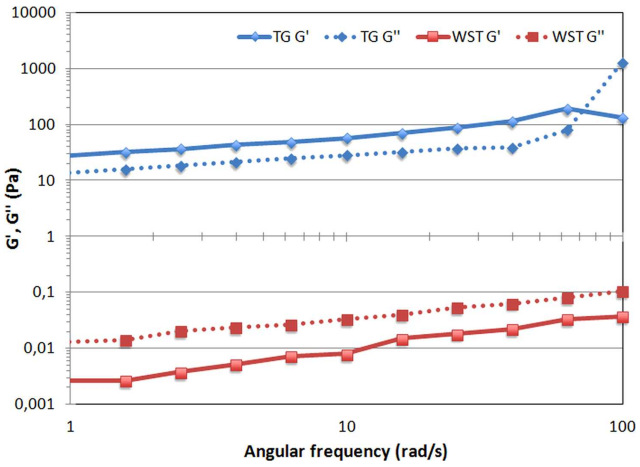

Figure 6. Influence of angular frequency on the storage and loss moduli of TG and WST. [Color figure can be viewed in the online issue, which is available at wileyonlinelibrary.com.]

Both raw TG suspension and WST solutions at different concentrations (up to 4%, w/v) cannot produce stable beads if dropped in the Ca^{2+} solution in a range of concentration of the gelling agent up to 1.5% w/v. This result represents an important difference with other polyuronic acids, which can typically form gels in the presence of calcium ions.

Fe^{3+} and Zn^{2+} were able to crosslink WST (Table III). Although bearing the same coordination number, zinc and calcium chloride show different ability to crosslink WST, only zinc being able to form a stable gel. This result is in agreement with results of other similar polysaccharides, where zinc ions can produce more stable pectinate gels than calcium ions.[40] In alginates, zinc ions can crosslink both guluronic acid (G) and mannuronic acid (M) and form GG, MM, and MG linkages while calcium ions can produce only GG linkages.[41]

Table II. Parameters Obtained Fitting the Viscosity Experimental Data with Carreau and Cross Models

Carreau model	η_0 (Pa s)	η_∞ (Pa s)	τ_{CA} (s)	M	R^2
TG	180.79	0.03	50.72	0.65	0.99
WST	0.09	0.02	8.78	0.91	0.97
Cross model	η_0 (Pa s)	η_∞ (Pa s)	τ_{CR} (s)	m	R^2
TG	160.71	0.05	33.44	0.67	0.99
WST	1.92	0.02	3.30E+08	0.28	0.99

Table III. Gelling Behavior of TG and WST in the Presence of Metallic Ions

Polymer concentration	Gelling agent			Results
(w/v)	Type	(w/v)	mM	
1%	$FeCl_3$	0.062%	3.9	Unstable spherical bead
		0.125%	7.7	Stable spherical bead
		0.250%	15.4	Stable spherical bead
		0.500%	30.8	Stable spherical bead
		1.000%	61.6	Stable spherical bead
1–2%	$ZnCl_2$	1.000%	73.3	Stable spherical bead
		2.000%	146.6	Unstable spherical bead
		3.000%	220.0	Unstable bead
		4.000%	293.2	Unstable bead

Spherical beads were observed when 1% WST solution was dropped into Fe^{3+} solution over a critical concentration ($\geq$0.125% v/w $FeCl_3$). Zinc was less effective than ferric ion as crosslinking agents at higher concentration ($\geq$1% v/w) and longer curing times are necessary to produce stable macrospheres. Moreover, increasing the Zn^{2+} concentration to 2–4% w/v resulted in beads with outer thin shells and liquid cores that tended to be disrupted during the washing steps. As reported in literature, Zn^{2+} crosslinked pectins[42,43] possess lower water content if compared to pectin gels obtained from other cations. The obtained results can be consistent with an outer shell characterized by reduced water content if compared to Fe^{3+} crosslinked beads, thus slowing or preventing the penetration of the ions in the core of the beads. The increase of concentration was only effective in a faster production of a Zn crosslinked surface of the bead. According to these observations, only Fe-WST was further studied.

Structural Characterization of the Beads

As ferric ions replace sodium ions in the WST sodium salt, the charge density, radius, and atomic weight of the cation are changed, creating a new environment around the carboxyl group.[44–46] Accordingly, results, reported in Table I and Figure 3(a,b), indicate peak shifts and modifications mainly in the bands relative to carboxyl group, namely asymmetric and symmetric stretching of carboxylate group and twisting band of CH_2. Other minor structural modifications are observed in the FTIR spectrum of Fe/WST, for example, symmetric deformation of —O—CH_3 groups in methyl esters shows a doublet at 1375 and 1359 cm^{-1}, that was a single band for TG at 1368 cm^{-1}.

Morphology of the Beads

Figure 7(a) shows spherical, narrow distribution of the size of the beads obtained by a digital camera. SEM images of lyophilized beads, showing surface and internal morphology are reported in Figure 7b–d.

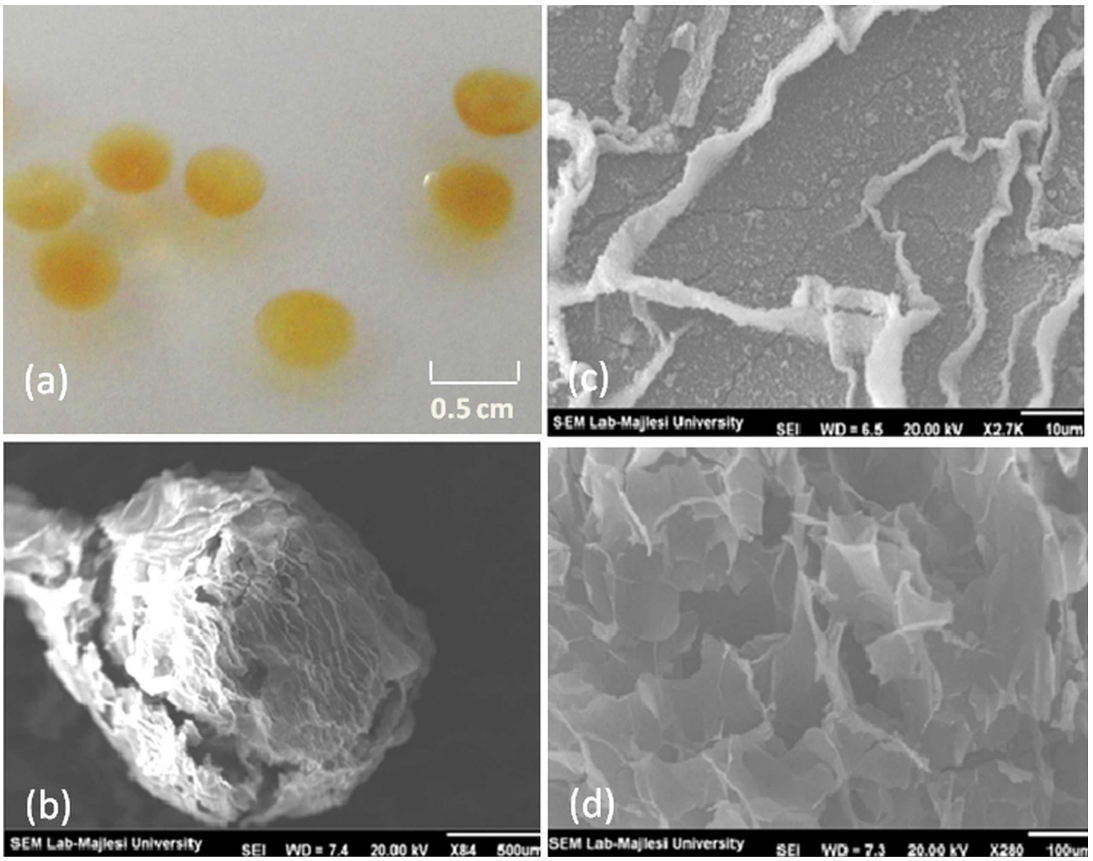

Figure 7. (a) Optical image of beads, (b) SEM image of bead, (c) SEM image of surface of bead, (d) SEM image of internal structure of bead. Beads were prepared by 1% WST and 0.5% ferric chloride. [Color figure can be viewed in the online issue, which is available at wileyonlinelibrary.com.]

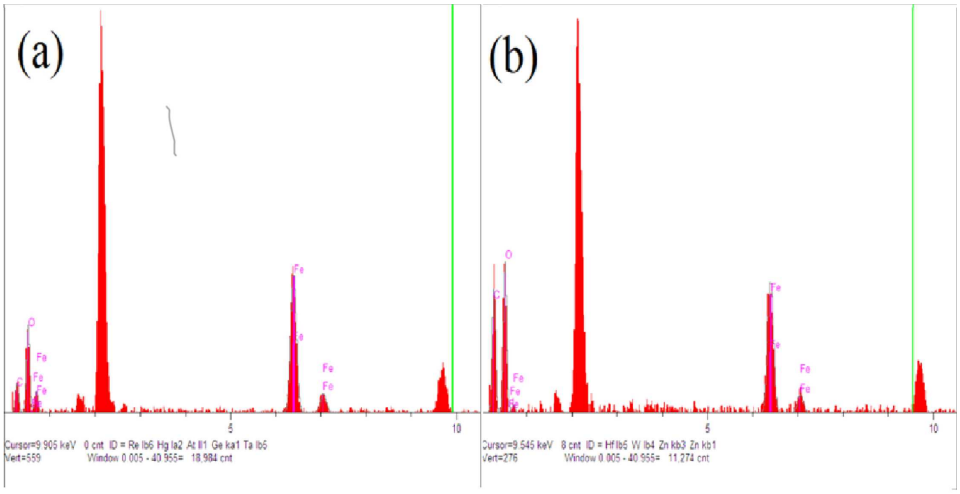

	Units	Conc	Error -2sig	Intensity (c/s)	Line	Elt.
	wt%.	20.135	3.831	36.71	Ka	C
	wt%.	34.162	6.440	103.72	Ka	O
	wt%.	45.703	10.897	297.00	Ka	Fe
Total	wt%.	100.000				

	Units	Conc	Error -2sig	Intensity (c/s)	Line	Elt.
	wt%.	33.899	5.561	77.36	Ka	C
	wt%.	42.567	5.939	88.24	Ka	O
	wt%.	23.533	7.450	138.83	Ka	Fe
Total	wt%.	100.000				

Figure 8. EDX analysis of ferric crosslinked WST beads: (a) surface of beads, (b) internal part. [Color figure can be viewed in the online issue, which is available at wileyonlinelibrary.com.]

Lyophilization may have induced changes in the morphology, in the intermolecular bonds and in the porosity. The samples analyzed by SEM are indeed different from the swollen samples, but still information can be gained from the comparison of the micrographs of the beads, lyophilized in the same conditions, as the sublimation of water is leaving a porosity which is somehow related to the different water distribution in the wet samples. This is giving, indirectly, information about the different characteristics of the gels that can be obtained from WST.

No microporosity can be observed on the surface (Figure 7c), indicating a low water content prior lyophilization of the beads. The internal part of beads is highly porous (Figure 7d). As shown in EDX analysis, the amount of ferric ions in internal part is almost two times more concentrated than in the interior part (Figure 8). These observations are pursuant to a high crosslinking degree on the surface of the beads resulting in low water content, while a less crosslinked gel, that contains higher amount of water in the interior part, could account the higher porosity resulting from lyophilization. Some cracks are observable on the surface (Figure 7b) suggesting again the different water content, which may be connected with a higher volume expansion during the freezing process in comparison to the surface of the bead. The inhomogeneous water content of the inner and outer layer can be considered an interesting characteristic to be further investigated to control the thickness of the outer layer affecting drug loading and release profiles. Higher water content in the inner part can also be positively considered for cell encapsulation. Data regarding Zn-crosslinked beads indicates that the effect of the cation concentration can modify this characteristic.

Cytotoxicity and Cell Adhesion

Viability data of L929, Hela, and HepG2 cells (cultivated with RPMI-1640) at 72 h are shown in Figure 9. To investigate cell viability, WST cytotoxicity on two cancerous cell lines of Hela

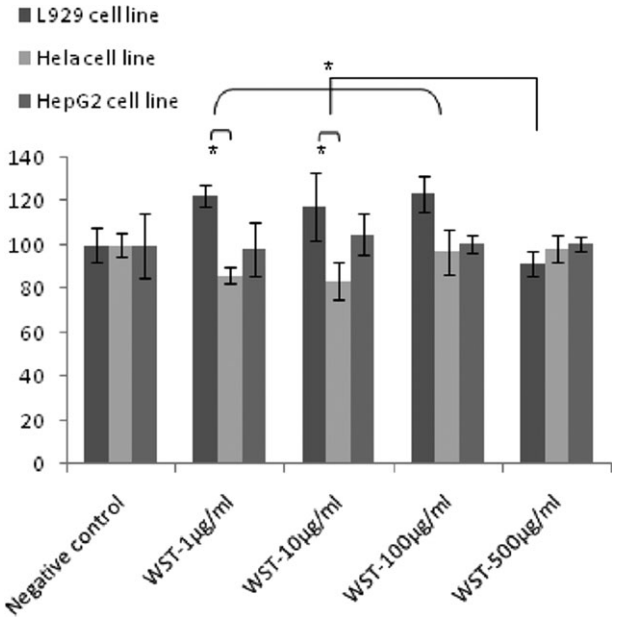

Figure 9. Relative cell viability of WST solution on L929 cells, Hela cells, and HepG2 cells. The relative cell viability read for the control (tissue culture polystyrene from culture plates) after 72 h of incubation was taken as the reference (100%). Significance was calculated by ANOVA ($*p \leq 0$).

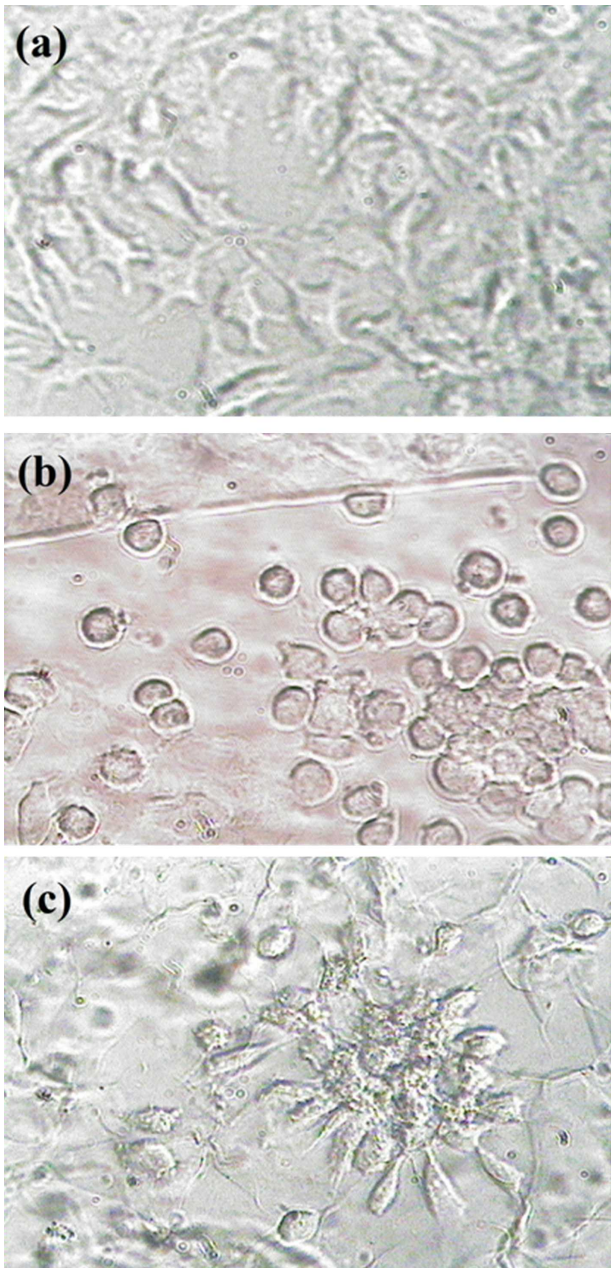

Figure 10. Cell adhesion of L929 on (a) cell culture plate, (b) ferric alginate film, (c) ferric crosslinked WST film. Images were acquired by reverse phase microscope (Olympus IX70). [Color figure can be viewed in the online issue, which is available at wileyonlinelibrary.com.]

and HepG2, and a fibroblast cell line of L929 has been assayed. WST has shown no toxicity either in Hela and HepG2 as cancerous cell lines or in L929 normal cell line. Cell viability of L929 cells was slightly improved in concentration of 1–100 μg/ml, and there are significant differences between viability of L929 and Hela cell lines in 1 and 10 μg/ml. By comparing viability of HepG2 with Hela cells no significant differences can be detected between HepG2 which expose asialoglycoprotein-receptors (ASGP-R) and galactose receptor and Hela, which does not express ASGP-R. Therefore, cells owing different characteristics are compatible with WST.

One of the main disadvantages of anionic polysaccharides in cell and tissue engineering is poor cell adhesion. L929 adhered on ferric crosslinked WST films with morphology similar to the culture plate. Ferric crosslinked alginate films, as control, showed a round morphology indicating poor cell adhesion (Figure 10). Considering spherical cells as nonadhered cells, the mean percentage of adhered cells was 10% and 50% for alginate gel and WST gel, respectively. The better cell adhesion of WST can be attributed to different interactions of cells with the specific side chain sugars of tragacanth.

CONCLUSIONS

In this study, a procedure was set up to prepare WST by de-esterification of TG, while retaining a high molecular weight and the main structural characteristics of raw TG and overcoming some of its typical limitations such as poor solubility and a limited ability to form water stable gels. Evaluation of WST cytotoxicity on Hela, HepG2, and L929 indicated lack of toxicity on these cell lines even at relatively high concentrations (500 μg/mL). WST was able to gel, and its gelling behavior is strictly dependent of the counter ion type. Among ferric, zinc, and calcium cations, ferric could interact with WST strongly thus making a stable hydrogel. Unlike pectin and alginate, well-known anionic polysaccharides, WST was not able to form hydrogels with calcium ions. This different behavior toward the different counter ions to promote ionotropic gelation could be related to the content and distribution, along the high molecular weight chains, of carboxylic acids available for ionic crosslinking and a specific branching, which can hinder the accessibility of these groups. Cell adhesion study proved cell adhesion ability of WST crosslinked with ferric ions. These properties of WST all together make this material a potential candidate for cell/tissue engineering, and future studies might highlight its applications also in the field of controlled drug delivery.

ACKNOWLEDGMENTS

The authors gratefully acknowledge Monica Moscatelli for GPC analyses and Marco Coletti for the support in the interpretation of the rheological analysis.

REFERENCES

1. Liu, Z.; Jiao, J.; Wang, Y.; Zhou, C.; Zhang, Z. *Adv. Drug Deliv. Rev.* **2008**, *60*, 1650.
2. Munarin, F.; Petrini, P.; Tanzi, M. C.; Barbosa, M. A.; Granja, P. L. *Soft Matter* **2012**, *8*, 4731.
3. Mano, J.; Silva, G.; Azevedo, H.; Malafaya, P.; Sousa, R.; Silva, S.; Boesel, L.; Oliveira, J.; Santos, T.; Marques, A. *J. R. Soc. Interface* **2007**, *4*, 999.
4. Rana, V.; Rai, P.; Tiwary, A. K.; Singh, R. S.; Kennedy, J. F.; Knill, C. J. *Carbohydr. Polym.* **2011**, *83*, 1031.
5. Verbeken, D.; Dierckx, S.; Dewettinck, K. *Appl. Microbiol. Biotechnol.* **2003**, *63*, 10.
6. Thimma, R. T.; Tammishetti, S. *J. Appl. Polym. Sci.* **2001**, *82*, 3084.

7. Munarin, F.; Petrini, P.; Farè, S.; Tanzi, M. C. *J. Mater. Sci.: Mater. Med.* **2010**, *21*, 365.
8. Munarin, F.; Guerreiro, S.; Grellier, M.; Tanzi, M. C.; Barbosa, M. A.; Petrini, P.; Granja, P. L. *Biomacromolecule* **2011**, *12*, 568.
9. Munarin, F.; Tanzi, M. C.; Petrini, P. *Int. J. Biol. Macromol.* **2012**, *51*, 681.
10. Gazori, T.; Khoshayand, M.; Azizi, E.; Yazdizade, P.; Nomani, A.; Haririan, I. *Carbohydr. Polym.* **2009**, *77*, 599.
11. Augst, A. D.; Kong, H. J.; Mooney, D. J. *Macromol. Biosci.* **2006**, *6*, 623.
12. El-Sherbiny, I. M. *Carbohydr. Polym.* **2010**, *80*, 1125.
13. Mura, C.; Manconi, M.; Valenti, D.; Manca, M. L.; Dķez-Sales, O.; Loy, G.; Fadda, A. M. *Carbohydr. Polym.* **2011**, *85*, 578.
14. Oliveira, G. F.; Ferrari, P. C.; Carvalho, L. Q.; Evangelista, R. C. *Carbohydr. Polym.* **2010**, *82*, 1004.
15. Khajavi, R.; Pourgharbi, S.; Rashidi, A.; Kiumarsi, A. *Int. J. Eng.* **2004**, *17*, 201.
16. Balaghi, S.; Mohammadifar, M.; Zargaraan, A. *Food Biophys.* **2010**, *5*, 59.
17. Mirhosseini, H.; Amid, B. T. *Food Res. Int.* **2012**, *46*, 387.
18. Phillips, G. O.; Williams, P. A. Handbook of Hydrocolloids; CRC Press LLC: Boca Raton, FL, **2000**, p 231.
19. Mohammadifar, M. A.; Musavi, S. M.; Kiumarsi, A.; Williams, P. A. *Int. J. Biol. Macromol.* **2006**, *38*, 31.
20. Seaman, J.; Davidson, R. Handbook of Water Soluble Gums and Resins; Mc Graw-Hill Book Company: New York, **1980**.
21. Aspinall, G.; Baillie, J. *J. Chem. Soc.* **1963**, *1963*, 1702.
22. Kaffashi, B.; Zandieh, A.; Khadiv-Parsi, P. *Macromol. Symp.* **2006**, *239*, 120.
23. Siahi, M. R.; Barzegar-Jalali, M.; Monajjemzadeh, F.; Ghaffari, F.; Azarmi, S. *AAPS Pharm. Sci. Tech.* **2005**, *6*, 626.
24. Cevik, A. G. S *J. Microencaps.* **2000**, *17*, 565.
25. Moghbel, A.; Naji, M. *Sci. Med. J.* **2008**, *7*, 274.
26. Kiani, A.; Shahbazi, M.; Asempour, H. *J. Appl. Polym. Sci.* **2012**, *1*, 99.
27. Kiani, A.; Asempour, H. *J. Appl. Polym. Sci.* **2012**, *126*, E478.
28. Cho, C.; Seo, S.; Park, I.; Kim, S.; Kim, T.; Hoshiba, T.; Harada, I.; Akaike, T. *Biomaterials* **2006**, *27*, 576.
29. Deters, A. M.; Lengsfeld, C.; Hensel, A. *J. Ethnopharmacol.* **2005**, *102*, 391.
30. Robert, L.; Fodil-Bourahla, I.; Bizbiz, L.; Robert, A. *Biomed. Pharmacother.* **2004**, *58*, 123.
31. Munarin, F.; Petrini, P.; Bozzini, S.; Tanzi, M. C. *J. Appl. Biomater. Function. Mater.* **2012**, *10*, 67.
32. Yoo, S-H.; Fishman, M. L.; Hotchkiss, A. T., Jr.; Lee, H. G. *Food Hydrocoll.* **2006**, *20*, 62.
33. Ghaffari, A.; Navaee, K.; Oskoui, M.; Bayati, K.; Rafiee-Tehrani, M. *Eur. J. Pharm. Biopharm.* **2007**, *67*, 175.
34. Yoo, H.; Park, T. *J. Control Release* **2001**, *70*, 63.
35. Yokoyama, M.; Okano, T.; Sakurai, Y.; Suwa, S.; Kataoka, K. *J. Control Release* **1996**, *39*, 351.
36. Kacurakova, M.; Capek, P.; Sasinkova, V.; Wellner, N.; Ebringerova, A. *Carbohydr. Polym.* **2000**, *43*, 195.
37. Chenlo, F.; Moreira, R.; Silva, C. *J. Food Eng.* **2010**, *96*, 107.
38. Balaghi, S.; Mohammadifar, M. A.; Zargaraan, A. *Food Biophys.* **2010**, *5*, 59.
39. Balaghi, S.; Mohammadifar, M. A.; Zargaraan, A.; Gavlighi, H. A.; Mohammadi, M. *Food Hydrocolloid* **2011**, *25*, 1775.
40. Das, S.; Chaudhury, A.; Ng, K. Y. *Int. J. Pharm.* **2011**, *406*, 11.
41. Jay, S. M.; Saltzman, W. M. *J. Control Release* **2009**, *134*, 26.
42. Kawadkar, J.; Meenakshi, K. C.; Ram, A. DARU *J. Pharm. Sci.* **2010**, *18*, 211.
43. Goh, C. H.; Heng, P. W. S.; Chan, L. W. *Carbohydr. Polym.* **2012**, *88*, 1.
44. Pathak, T.; Yun, J.; Lee, J.; Paeng, K. *Carbohydr. Polym.* **2010**, *81*, 633.
45. Assifaoui, A.; Loupiac, C.; Chambin, O.; Cayot, P. *Carbohydr. Res.* **2010**, *345*, 929.
46. Papageorgiou, S.; Kouvelos, E.; Favvas, E.; Sapalidis, A.; Romanos, G.; Katsaros, F. *Carbohydr. Res.* **2010**, *345*, 469.